Morales-Herrera, S., Jourquin, J., Coppe, F., Lopez-Galvis, L., De Smet, T., Safi, A., Njo, M., Griffiths, C. A., Sidda, J. D., Mccullagh, J. S. O., Xue, X., Davis, B. G., Van der Eycken, J., Paul, M. J., Van Dijck, P. and Beeckman, T. 2023. Trehalose-6-phosphate signaling regulates lateral root formation in Arabidopsis thaliana. *Proceedings of the National Academy of Sciences.* 120 (40), p. e2302996120. https://doi.org/10.1073/pnas.2302996120

PNAS

Supporting Information for

Trehalose-6-phosphate signaling regulates lateral root formation in Arabidopsis thaliana

Stefania Morales-Herrera, Joris Jourquin, Frederic Coppé, Lorena Lopez-Galvis, Tom De Smet, Alaeddine Safi, Maria Njo, Cara A. Griffiths, John D. Sidda, James S.O. Mccullagh, Xiaochao Xue, Benjamin G. Davis, Johan Van der Eycken, Matthew J. Paul, Patrick Van Dijck, Tom Beeckman

Corresponding author: Tom Beeckman
Email: tobee@psb.ugent.be

This PDF file includes:

Supporting Information Text

Supplementary Materials and Methods

T6P and T4P synthesis

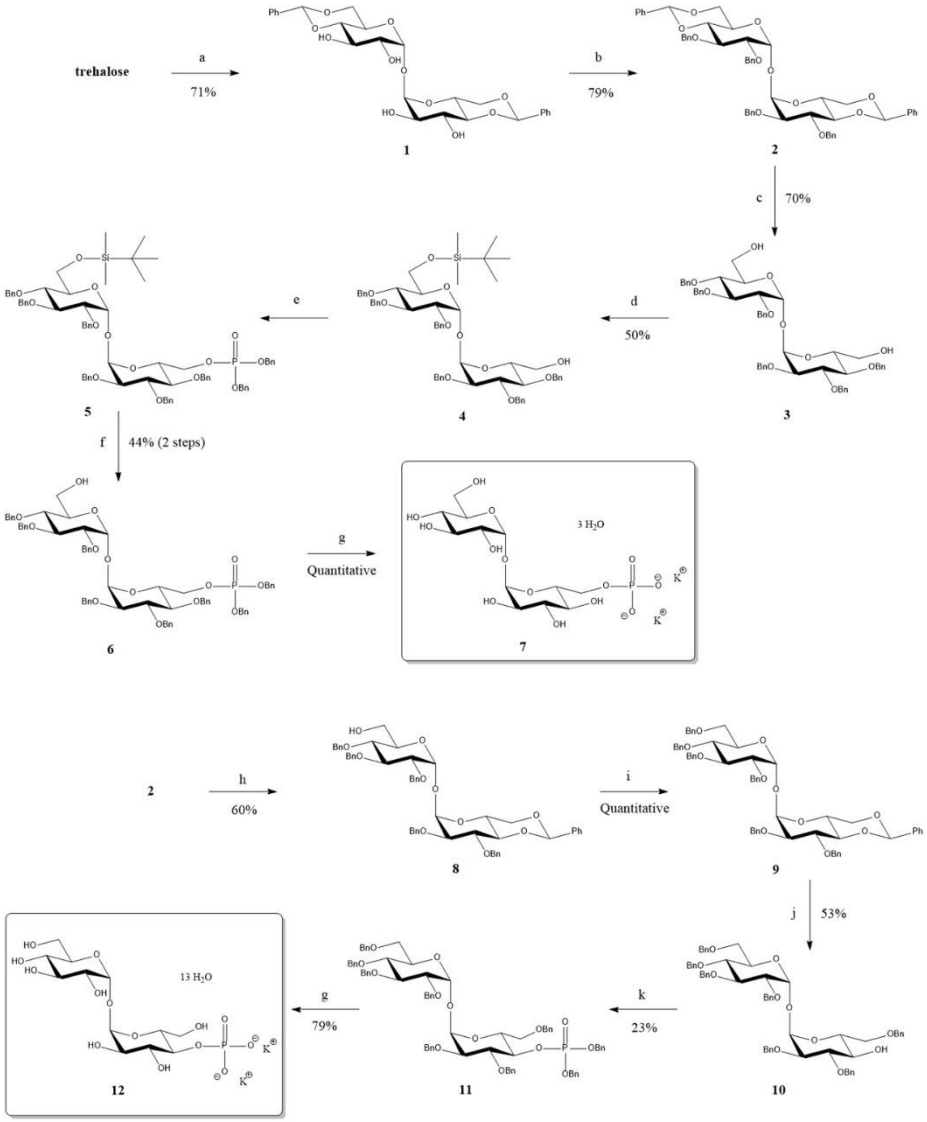

Figure S1: Synthesis of T6P and T4P. Reagents and conditions: (a) 0.05 eq camphorsulfonic acid, 2.2 eq benzaldehyde dimethyl acetal, DMF, 90 °C, 30 min; (b) 10 eq NaH, 8 eq BnBr, 0.2 eq TBAI, DMF, 0 °C-rt, 48 h; (c) 7 eq DIBAL-H, toluene, 0 °C-rt, o.n.; (d) 1.5 eq imidazole, 1 eq tert-butyldimethylsilyl chloride, 24 h; (e) 10 eq PCl_3, 32 eq Et_3N, 60 eq BnOH, 120 eq pyridine, 60 eq acetic anhydride, H_2O_2, diethyl ether, 0°C-rt, 168 h; (f) 3 eq TBAF, THF, o.n.; (g) 1) 0.1 eq Pd/C, EtOAc/MeOH 2/5, 48 h; 2) 2 eq KOH, H_2O; (h) 5 eq DIBAL-H, toluene, -18 °C-rt, 1.5 h; (i) 2.5 eq NaH, 4 eq BnBr, DMF, 0 °C-rt, o.n.; (j) 5 eq DIBAL-H, CH_2Cl_2, 0 °C, 3 h; (k) 10 eq PCl_3, 32 eq Et_3N, 60 eq BnOH, 120 eq pyridine, 60 eq acetic anhydride, H_2O_2, diethyl ether, 0°C-rt, 192 h

General

All reactions, unless otherwise stated, were carried out under argon atmosphere in dry solvents. Dichloromethane and triethylamine were freshly distilled from CaH_2. Toluene was freshly distilled from Na. Tetrahydrofuran and diethyl ether were freshly distilled from Na/benzophenone. Other solvents and reagents were obtained from commercial sources and were used as received without further purification. Flash chromatography was carried out with Rocc silicagel 60 Å, 40-63 mm. Precoated silica gel plates (Macherey-Nagel SIL G-25 UV254) were used for TLC employing UV-absorption at 254nm and $Mo_7O_{24}/Ce(SO_4)_2/aq.H_2SO_4$ staining for visualization. Preparative HPLC was performed on a Phenomenex Luna C18 (2) (5 µm, 220 x 21.20 mm) column. Electrospray mass spectra were recorded on an Agilent 1100 series single quadrupole MS detector type VL with an APCI source and an API-ES source, provided with a Phenomenex Luna C18 (2) (5 µm, 250mm x 4.60mm) column. High resolution mass spectrometry (HRMS) was performed on an Agilent 1100 series connected to a 6220 A TOF-MS detector equipped with an APCI-ESI multimode source. ^{1}H-NMR and ^{13}C-NMR spectra were recorded on a Bruker Avance 300, Bruker Avance 400 or a Bruker AM 500 spectrometer as indicated with chemical shifts reported in parts per million, referenced to the residual solvent signals (D_2O: 4.75 ppm, CD_3OD: 3.31 and 49.15 ppm, benzene-d_6: 7.16 and 128.0 ppm). ^{13}C-NMR Spectra recorded in D_2O were referenced to the methyl signal (30.89 ppm) of acetone (1 drop added). Coupling constants (J) are reported in hertz (Hz).

4,6,4',6'-Di-O-benzylidene-α,α-D-trehalose (1)

Anhydrous trehalose (30 g, 87.6 mmol) and camphorsulfonic acid (1 g, 4.4 mmol) were suspended in DMF (175 ml). Benzaldehyde dimethyl acetal (28.2 ml, 192.8 mmol) was added. The flask was attached to a rotary evaporator and heated to 90°C at atmospheric pressure for 15 min, then to a rotary evaporator at 60°C at reduced pressure for 15 min to remove the methanol formed. A second amount of benzaldehyde dimethyl acetal (28.2 ml, 192.8 mmol) was added. The flask was once more attached to a rotary evaporator at 90°C at atmospheric pressure for 15 min. The reaction was quenched with triethylamine (14 ml). The volatiles were removed via co-evaporation with toluene

under reduced pressure. The crude mixture was recrystallized from H_2O/EtOH 7/4 affording compound **1** as white crystals in a yield of 71% (32.1 g, 61.9 mmol).

ESMS [m/z (fragment, intensity), API-ES positive mode]: 519.2 ($M+H^+$, 100). HRMS (ESI-TOF): calculated for $C_{26}H_{31}O_{11}^+$ $[M+H]^+$ 518.1788; found 519.1850.

^{1}H NMR (400 MHz, Methanol-d_4) δ 7.55 – 7.47 (m, 4H), 7.41 – 7.31 (m, 6H), 5.59 (s, 2H), 5.15 (d, *J* = 3.9 Hz, 2H), 4.24 (dd, *J* = 10.0, 5.0 Hz, 2H), 4.14 (ddd, *J* = 9.9, 9.9, 4.9 Hz, 2H), 4.05 (dd, *J* = 9.4, 9.4 Hz, 2H), 3.75 (dd, *J* = 10.1, 10.1 Hz, 2H), 3.65 (dd, *J* = 9.4, 3.9 Hz, 2H), 3.51 (dd, *J* = 9.5, 9.5 Hz, 2H) ppm.

^{13}C NMR (101 MHz, Methanol-d_4) δ 139.3 (C) 129.9 (CH), 129.1 (CH), 127.6 (CH), 103.1 (CH), 96.5 (CH), 83.1 (CH), 73.8 (CH), 71.5 (CH), 70.0 (CH_2), 64.2 (CH) ppm.

2,3,2',3'-Tetra-O-benzyl-4,6,4',6'-Di-O-benzylidene-α,α-D-trehalose (2)

To a stirred solution of **1** (32.1 g, 61.9 mmol) in anhydrous DMF (250 ml) at room temperature, NaH (60% suspension in mineral oil, 24.7 g, 619 mmol) was slowly added, resulting in hydrogen gas formation. The reaction mixture was cooled to 0°C. Benzyl bromide (58.9 ml, 494.9 mmol) was added dropwise followed by tetra-n-butylammonium iodide (TBAI) (4.57 g, 12.4 mmol). The reaction mixture was stirred at room temperature for two days. The mixture was then cooled to 0°C, quenched with MeOH (100 ml) and concentrated under reduced pressure. The crude mixture was diluted with EtOAc (500 ml) and transferred to a separation funnel. The organic phase was washed with brine (3 x 500 ml), dried over $MgSO_4$, filtered and concentrated under reduced pressure. The crude product was purified by column chromatography (gradient elution: hexane/EtOAc 85/15 to 60/40) giving the title compound **2** as white crystals in a yield of 79 % (42.9 g, 488 mmol).

ESMS [m/z (fragment, intensity), API-ES positive mode]: 896.3 ($M+NH_4^+$, 100). HRMS (ESI-TOF): calculated for $C_{54}H_{58}NO_{11}^+$ $[M+NH_4]^+$ 896.4010; found 896.4003.

^{1}H NMR (400 MHz, Benzene-d_6) δ 7.75 – 7.67 (m, 4H), 7.49 – 7.43 (m, 8H), 7.36 – 7.13 (m, 18H), 5.50 (s, 2H), 5.37 (d, *J* = 3.8 Hz, 2H), 5.05 (d, *J* = 11.6 Hz, 2H), 4.85 (d, *J* = 11.8 Hz, 2H), 4.81 (d,

J = 11.5 Hz, 2H), 4.70 (d, *J* = 11.8 Hz, 2H), 4.65 (ddd, *J* = 10.0, 10.0, 4.8 Hz, 2H), 4.48 (dd, *J* = 9.3, 9.3 Hz, 2H), 4.33 (dd, *J* = 10.1, 4.9 Hz, 2H), 3.68 (dd, *J* = 9.4 Hz, 2H), 3.66 (dd, *J* = 10.2 Hz, 2H) ppm.

^{13}C NMR (101 MHz, Benzene-d_6) δ 139.7 (C), 138.8 (C), 138.5 (C), 129.0 (CH), 128.8 (CH), 128.4 (CH), 127.9 (CH), 127.5 (CH), 126.8 (CH), 101.7 (CH), 94.7 (CH), 83.0 (CH), 79.4 (CH), 75.4 (CH_2), 74.4 (CH_2), 69.3 (CH_2), 63.5 (CH) ppm.

2,3,4,2',3',4'-Hexa-O-benzyl-α,α-D-trehalose (3)

A solution of **2** (10.5 g, 11.9 mmol) in toluene (119 ml) was cooled to -18°C. DIBAL-H (1M in toluene, 83.3 ml, 83.3 mmol) was added dropwise. The reaction mixture was stirred overnight at room temperature. After cooling to 0°C, subsequently MeOH (21 ml) and KOH (10% in H_2O, 7 ml) were cautiously added. The mixture was transferred to a separation funnel containing a saturated aqueous solution of Rochelle salt (400 ml). The aqueous layer was extracted with CH_2Cl_2 (3 x 400 ml). The combined organic layers were dried over $MgSO_4$. The drying agent was filtered and the filtrate was concentrated under reduced pressure. The crude product was purified by column chromatography (gradient elution: hexane/EtOAc 70/30 to 55/45) giving the title compound **3** as a colorless oil in a yield of 70 % (7.3 g, 8.3 mmol).

ESMS [m/z (fragment, intensity), API-ES positive mode]: 900.4 ($M+NH_4^+$, 100). HRMS (ESI-TOF): calculated for $C_{56}H_{61}O_{13}^-$ $[M+OAc]^-$ 941.4118; found 941.4114.

^{1}H NMR (400 MHz, Benzene-d_6) δ 7.47 – 7.41 (m, 8H), 7.39 – 7.31 (m, 4H), 7.30 – 7.14 (m, 18H), 5.42 (d, J = 3.6 Hz, 2H), 5.06 (d, *J* = 11.3 Hz, 2H), 5.02 (d, *J* = 11.2 Hz, 2H).4.88 (d, J = 11.3 Hz, 2H), 4.78 (d, J = 11.3 Hz, 2H), 4.73 (s, 4H), 4.49 – 4.37 (m, 4H), 3.91 – 3.76 (m, 6H), 3.68 (dd, J = 9.6, 3.6 Hz, 2H), 1.94 (s, 2H) ppm.

^{13}C NMR (101 MHz, Benzene-d_6) δ 139.7 (C), 139.1 (C), 138.7 (C), 128.7 (CH), 128.5 (CH), 128.5 (CH), 128.1 (CH), 128.0 (CH), 127.9 (CH), 127.9 (CH), 127.8 (CH), 127.6 (CH), 93.4 (CH), 82.3 (CH), 80.0 (CH), 78.3 (CH), 75.5 (CH_2), 75.0 (CH_2), 73.4 (CH_2), 72.2 (CH), 62.2 (CH_2) ppm.

2,3,4,2',3',4'-Hexa-O-benzyl-6'-O-(tert-butyldimethylsilyl)-α,α-D-trehalose (4)

To a solution of **3** (4.65 g, 5.3 mmol) in anhydrous DMF (53 ml), imidazole (540 mg, 7.9 mmol) and tert-butyldimethylsilyl chloride (790 mg, 5.3 mmol) were added. The reaction mixture was stirred for 24 h at room temperature. After quenching with H_2O (15 ml), the mixture was transferred to a separation funnel containing H_2O (400 ml). The aqueous layer was extracted with EtOAc (2 x 400 ml). The combined organic layers were dried over $MgSO_4$. The drying agent was filtered and the filtrate was concentrated under reduced pressure. The crude product was purified by column chromatography (gradient elution: hexane/EtOAc 90/10 to 45/55) giving the title compound **4** as a colorless oil in a yield of 50 % (2.59 g, 2.6 mmol).

ESMS [m/z (fragment, intensity), API-ES positive mode]: 1014.3 ($M+NH_4^+$, 100). HRMS (ESI-TOF): calculated for $C_{60}H_{76}NO_{11}Si^+$ $[M+NH_4]^+$ 1014.5188; found 1014.5215.

^{1}H NMR (400 MHz, Benzene-d_6) δ 7.25 – 7.15 (m, 10H), 7.12 – 6.91 (m, 20H), 5.23 (d, *J* = 3.6 Hz, 1H), 5.19 (d, *J* = 3.6 Hz, 1H), 4.93 (d, *J* = 11.3 Hz, 1H), 4.85 (d, *J* = 11.3 Hz, 1H), 4.81 (d, *J* = 11.4 Hz, 1H), 4.77 (d, *J* = 11.3 Hz, 1H), 4.69 (d, *J* = 11.3 Hz, 1H), 4.68 (d, *J* = 11.3 Hz, 1H), 4.63 (d, *J* = 11.4 Hz, 1H), 4.55 – 4.50 (m, 3H), 4.40 (d, *J* = 3.4 Hz, 2H), 4.31 – 4.19 (m, 3H), 4.17 (dt, *J* = 10.0, 3.4 Hz, 1H), 3.82 – 3.70 (m, 3H), 3.61 – 3.49 (m, 4H), 3.42 (dd, *J* = 9.6, 3.6 Hz, 1H), 0.89 (s, 9H), 0.02 (s, 3H) , 0.00 (s, 3H) ppm.

^{13}C NMR (101 MHz, Benzene-d_6) δ 139.8 (C), 139.7 (C), 139.5 (C), 139.2 (C), 138.9 (C), 138.7 (C), 128.7 (CH), 128.6 (CH), 128.5 (CH), 128.5 (CH), 128.5 (CH), 128.0 (CH), 128.0 (CH), 127.9 (CH), 127.7 (CH), 127.7 (CH), 127.5 (CH), 93.5 (CH), 93.3 (CH), 82.4 (CH), 82.3 (CH), 80.5 (CH), 80.3 (CH), 78.3 (CH), 78.3 (CH), 75.7 (CH_2), 75.5 (CH_2), 75.1 (CH_2), 75.0 (CH_2), 73.4 (CH_2), 73.3 (CH_2), 72.5 (CH), 72.0 (CH), 62.7 (CH_2), 62.1 (CH_2), 26.2 (CH_3), 18.7 (C), -4.9 (CH_3), -5.1 (CH_3) ppm.

2,3,4,2',3',4'-Hexa-O-benzyl-6-(dibenzyl phosphate)-6'-O-(tert-butyldimethylsilyl)-α,α-D-trehalose (5) and 2,3,4,2',3',4'-Hexa-O-benzyl-6-(dibenzyl phosphate)-α,α-D-trehalose (6)

To a cooled (0°C) solution of phosphorus trichloride (2.27 ml, 26 mmol) in diethyl ether (160 ml), triethylamine (11.6 ml, 83.1 mmol) was added dropwise. A solution of **4** (2.6 g, 2.6 mmol) in diethyl ether (100 ml) was added. The reaction mixture was stirred for 30 min at 0°C, then for 24 h at room temperature. The reaction mixture was then cooled to 0°C and benzyl alcohol (16.2 ml, 156 mmol) was added. The reaction mixture was stirred for 30 min at 0°C, then for 4 days at room temperature. Pyridine (25.1 ml, 312 mmol) and acetic anhydride (14.7 ml, 156 mmol) were added, after which the reaction mixture was stirred for 24 h. Subsequently, H_2O_2 (30% aq, 26 ml) was added, followed by stirring for 24h. The reaction mixture was then cooled to 0°C, and $Na_2S_2O_3$ (10% aq, 260 ml) was added. After stirring for 30 min at 0°C, the mixture was transferred to a separation funnel containing H_2O (250 ml). The organic phase was separated, after which the aqueous layer was extracted with CH_2Cl_2 (2 x 250 ml). The combined organic layers were dried over Na_2SO_4. The drying agent was filtered and the filtrate was concentrated under reduced pressure. The crude product was partly purified by column chromatography (gradient elution: hexane/EtOAc 100/0 to 60/40) yielding the title compound **5** as a mixture with tribenzyl phosphate.

The crude mixture of **5** and tribenzyl phosphate was dissolved in THF (26 ml). Tetra-n-butylammonium fluoride (1M in THF, 7.8 ml, 7.8 mmol) was added at room temperature. The reaction mixture was stirred overnight, and subsequently transferred to a separation funnel containing $KHSO_4$ (1M in H_2O, 250 ml). The aqueous layer was extracted with EtOAc (3 x 250 ml). The combined organic layers were dried over anhydrous Na_2SO_4. The drying agent was filtered and the filtrate was concentrated under reduced pressure. The crude product was purified by column chromatography (gradient elution: hexane/EtOAc 60/40 to 40/60) affording the title compound **6** as a colorless oil in a yield of 44 % (1.3 g, 1.2 mmol) over two steps.

(5) ESMS [m/z (fragment, intensity), API-ES positive mode]: 1274.4 ($M+NH_4^+$, 100).

(6) ESMS [m/z (fragment, intensity), API-ES positive mode]: 1160.3 ($M+NH_4^+$, 100). HRMS (ESI-TOF): calculated for $C_{68}H_{75}NO_{14}P^+$ $[M+NH_4]^+$ 1160.4925; found 1160.4921.

^{1}H NMR (400 MHz, Benzene-d_6) δ 7.46 – 7.10 (m, 40H), 5.47 – 5.39 (m, 2H), 5.13 – 4.98 (m, 8H), 4.90 – 4.65 (m, 8H), 4.56 – 4.51 (m, 1H), 4.50 – 4.34 (m, 5H), 3.93 – 3.74 (m, 4H), 3.67 – 3.63 (m, 2H) ppm.

^{31}P NMR (162 MHz, Benzene-d_6) δ 13.92 ppm.

^{13}C NMR (101 MHz, Benzene-d_6) δ 139.7 (C), 139.6 (C), 139.2 (C), 139.1 (C), 138.7 (C), 138.7 (C), 136.8 (d, *J* = 6.2 Hz, C), 136.7 (d, *J* = 5.5 Hz, C), 128.8 (CH), 128.8 (CH), 128.7 (CH), 128.5 (CH), 128.5 (CH), 128.2 (CH), 128.0 (CH), 127.9 (CH), 127.9 (CH), 127.7 (CH), 127.5 (CH), 127.5 (CH), 93.4 (CH), 93.3 (CH), 82.2 (CH), 82.2 (CH), 80.0 (CH), 79.9 (CH), 78.3 (CH), 77.7 (CH), 75.5 (CH_2), 75.5 (CH_2), 75.1 (CH_2), 75.0 (CH_2), 73.3 (CH_2), 73.2 (CH_2), 72.1 (CH), 70.6 (d, *J* = 7.5 Hz, CH), 69.4 (d, *J* = 5.1 Hz, CH_2), 66.8 (d, *J* = 5.5 Hz, CH_2), 62.2 (CH_2) ppm.

Trehalose-6-phosphate dipotassium salt trihydrate (7)

To a solution of **6** (574 mg, 0.502 mmol) in MeOH (5 ml) and EtOAc (2 ml), palladium on carbon (10%, 53 mg, 0.050 mmol) was added. A balloon containing H_2-gas was attached to the flask. The reaction mixture was stirred at room temperature for 2 days under H_2-atmosphere, and subsequently filtered over celite. The filtrate was concentrated under reduced pressure, affording trehalose-6-phosphate as a white powder in a quantitative yield (212 mg, 0.502 mmol).

To a solution of trehalose-6-phosphate (212 mg, 0.502 mmol) in H_2O (20 ml), KOH (0.05 M in H_2O, 20.1 ml) was added. The mixture was subjected to lyophilization, giving compound **7** (trehalose-6-phosphate dipotassium salt trihydrate) as a white powder in quantitative yield (278 mg).

ESMS [m/z (fragment, intensity), API-ES negative mode]: 421.1 ($M\text{-}2K^{+}+H^{+}$, 100). HRMS (ESI-TOF): calculated for $C_{12}H_{22}O_{14}P^{-}$ $[M\text{-}2K+H]^{-}$ 421.0753; found 421.0736.

^{1}H NMR (400 MHz, Deuterium Oxide) δ 5.18 (d, *J* = 3.9 Hz, 1H), 5.14 (d, *J* = 3.9 Hz, 1H), 3.99 (ddd, *J* = 11.8, 7.6, 4.1 Hz, 1H), 3.90 (ddd, *J* = 12.1, 5.5, 2.1 Hz, 1H), 3.87 – 3.82 (m, 2H), 3.82 – 3.75 (m, 4H), 3.74 – 3.69 (m, 1H), 3.68 – 3.55 (m, 3H), 3.41 (dd, J= 9.4, 9.4 Hz, 1H) ppm.

^{31}P NMR (162 MHz, Deuterium Oxide) δ 4.47 ppm.

^{13}C NMR (101 MHz, Deuterium Oxide) δ 93.4 (CH), 93.3 (CH), 72.4 (CH), 72.2 (CH), 72.1 (CH), 71.8 (d, *J* = 6.9 Hz, CH), 71.2 (CH), 70.9 (CH), 69.7 (CH), 69.1 (CH), 62.4 (d, *J* = 4.3 Hz, CH_2), 60.5 (CH_2) ppm.

2,3,4,2',3'-Penta-O-benzyl-4',6'-O-benzylidene-α,α-D-trehalose (8)

A solution of **2** (4.14 g, 4.70 mmol) in toluene (47 ml) was cooled to -18°C. DIBAL-H (1M in toluene, 23.5 ml, 23.5 mmol) was added dropwise. The reaction mixture was stirred for 1.5 h at room temperature. After cooling to 0°C, MeOH (8.2 ml) and KOH (10% aq, 2.7 ml) were cautiously added. The mixture was transferred to a separation funnel containing a saturated aqueous solution of Rochelle salt (300 ml). The aqueous layer was extracted with CH_2Cl_2 (3 x 300 ml). The combined organic layers were dried over $MgSO_4$. The drying agent was filtered and the filtrate was concentrated under reduced pressure. The crude product was purified by column chromatography (gradient elution: hexane/EtOAc 80/20 to 50/50) giving the title compound **8** as a white foam in a yield of 60 % (2.47 g, 2.80 mmol).

ESMS [m/z (fragment, intensity), API-ES positive mode]: 898.4 ($M+NH_4^+$, 100). HRMS (ESI-TOF): calculated for $C_{54}H_{60}NO_{11}^+$ $[M+NH_4]^+$ 898.4166; found 898.4149.

^{1}H NMR (400 MHz, Benzene-d_6) δ 7.76 – 7.69 (m, 2H), 7.47 – 7.41 (m, 8H), 7.38 – 7.13 (m, 20H), 5.51 (s, 1H), 5.39 (d, *J* = 3.7 Hz, 1H), 5.34 (d, *J* = 3.6 Hz, 1H), 5.07 (d, *J* = 11.6 Hz, 1H), 5.02 (d, *J* = 11.3 Hz, 1H), 5.01 (d, *J* = 11.3 Hz, 1H), 4.90 – 4.57 (m, 8H), 4.50 (dd, *J* = 9.3, 9.3 Hz, 1H), 4.47 – 4.39 (m, 2H), 4.35 (dd, *J* = 10.1, 4.9 Hz, 1H), 3.88 – 3.60 (m, 7H), 1.60 (s, 1H) ppm.

^{13}C NMR (101 MHz, Benzene-d_6) δ 139.7 (C), 139.7 (C), 139.2 (C), 138.8 (C), 138.7 (C), 138.5 (C), 129.0 (CH), 128.8 (CH), 128.7 (CH), 128.5 (CH), 128.5 (CH), 128.4 (CH), 128.0 (CH), 127.9 (CH), 127.7 (CH), 127.5 (CH), 101.7 (CH), 94.4 (CH), 93.6 (CH), 83.0 (CH), 82.2 (CH), 80.1 (CH), 79.4 (CH), 79.3 (CH), 78.2 (CH), 75.5 (CH_2), 75.3 (CH_2), 75.0 (CH_2), 74.1 (CH_2), 73.7 (CH_2), 72.1 (CH), 69.3 (CH_2), 63.5 (CH), 62.1 (CH_2) ppm.

2,3,4,6,2',3'-Hexa-O-benzyl-4',6'-O-benzylidene-α,α-D-trehalose (9)

To a solution of **8** (3.00 g, 3.41 mmol) in anhydrous DMF (7 ml) at room temperature, NaH (60% suspension in mineral oil, 304 mg, 8.51 mmol) was slowly added, resulting in hydrogen gas formation. The reaction mixture was cooled to 0°C, and benzyl bromide (1.62 ml, 13.62 mmol) was added dropwise. The reaction mixture was stirred overnight at room temperature, and subsequently cooled to 0°C and quenched with MeOH (3.2 ml). The crude mixture was diluted with EtOAc (70 ml) and transferred to a separation funnel. The organic phase was washed with brine (3 x 70 ml), dried over $MgSO_4$, filtered and concentrated under reduced pressure. The crude product was purified by column chromatography (gradient elution: hexane/EtOAc 85/15 to 75/25) giving the title compound **9** as a colorless oil in quantitative yield (3.31 g, 3.41 mmol).

ESMS [m/z (fragment, intensity), API-ES positive mode]: 988.3 ($M+NH_4^+$, 100). HRMS (ESI-TOF): calculated for $C_{61}H_{66}NO_{11}^+$ $[M+NH_4]^+$ 988.4636; found 988.4628.

^{1}H NMR (400 MHz, Benzene-d_6) δ 7.74 – 7.68 (m, 2H), 7.47 – 7.39 (m, 11H), 7.37 – 7.14 (m, 22H), 5.52 (d, *J* = 3.8 Hz, 1H), 5.49 (s, 1H), 5.45 (d, *J* = 3.6 Hz, 1H), 5.10 – 5.01 (m, 3H), 4.90 – 4.74 (m, 5H), 4.68 – 4.44 (m, 9H), 4.30 (dd, *J* = 10.2, 4.9 Hz, 1H), 3.82 – 3.76 (m, 2H), 3.73 (dd, *J* = 9.2, 3.8 Hz, 1H), 3.73 (dd, *J* = 9.7, 3.6 Hz, 1H), 3.70 – 3.61 (m, 2H), 1.48 (s, 1H) ppm.

^{13}C NMR (101 MHz, Benzene-d_6) δ 139.8 (C), 139.8 (C), 139.4 (C), 139.0 (C), 139.0 (C), 138.7 (C), 138.5 (C), 129.0 (CH), 128.8 (CH), 128.6 (CH), 128.5 (CH), 128.4 (CH), 128.4 (CH), 128.0 (CH), 128.0 (CH), 127.9 (CH), 127.9 (CH), 127.7 (CH), 127.6 (CH), 127.5 (CH), 126.8 (CH), 101.7 (CH), 94.4 (CH), 93.7 (CH), 83.0 (CH), 82.5 (CH), 80.4 (CH), 79.4 (CH), 79.4 (CH), 78.6 (CH), 75.5 (CH_2), 75.3 (CH_2), 75.0 (CH_2), 73.9 (CH_2), 73.7 (CH_2), 73.6 (CH_2), 71.7 (CH), 69.5 (CH_2), 69.3 (CH_2), 63.4 (CH) ppm.

2,3,4,6,2',3',6'-Hepta-O-benzyl-α,α-D-trehalose (10)

A solution of **9** (3.14 g, 3.24 mmol) in dry CH_2Cl_2 (2 ml) was cooled to 0°C. DIBAL-H (1M in CH_2Cl_2, 16.2 ml, 16.2 mmol) was added dropwise. The reaction mixture was stirred for 3 h at 0°C. MeOH

(8 ml) and KOH (10% in H_2O, 2.7 ml) were cautiously added. The mixture was transferred to a separation funnel containing a saturated aqueous solution of Rochelle salt (200 ml). The aqueous layer was extracted with CH_2Cl_2 (3 x 200 ml). The combined organic layers were dried over $MgSO_4$. The drying agent was filtered and the filtrate was concentrated under reduced pressure. The crude product was purified by column chromatography (gradient elution: hexane/EtOAc 90/10 to 65/35) giving the title compound **10** as a colorless oil in a yield of 53 % (1.66 g, 1.71 mmol).

ESMS [m/z (fragment, intensity), API-ES positive mode]: 990.4 ($M+NH_4^+$, 100). HRMS (ESI-TOF): calculated for $C_{61}H_{68}NO_{11}^+$ $[M+NH_4]^+$ 990.4792; found 990.4774.

^{1}H NMR (400 MHz, Benzene-d_6) δ 7.46 – 7.14 (m, 35H), 5.61 (d, *J* = 3.5 Hz, 1H), 5.60 (d, *J* = 3.6 Hz, 1H), 5.12 – 5.01 (m, 3H), 4.92 – 4.54 (m, 9H), 4.54 – 4.44 (m, 5H), 4.31 (dd, *J* = 9.2, 9.2 Hz, 1H), 3.95 – 3.71 (m, 7H), 3.68 (dd, *J* = 9.6, 3.6 Hz, 1H) ppm.

^{13}C NMR (101 MHz, Benzene-d_6) δ 139.9 (C), 139.8 (C), 139.5 (C), 139.0 (C), 138.9 (C), 138.9 (C), 128.6 (CH), 128.6 (CH), 128.6 (CH), 128.4 (CH), 128.0 (CH), 127.9 (CH), 127.8 (CH), 127.7 (CH), 127.7 (CH), 127.6 (CH), 127.5 (CH), 93.3 (CH), 82.4 (CH), 81.9 (CH), 80.2 (CH), 79.9 (CH), 78.6 (CH), 75.5 (CH_2), 75.3 (CH_2), 75.0 (CH_2), 73.8 (CH_2), 73.7 (CH_2), 73.0 (CH_2), 73.0 (CH_2), 72.2 (CH), 71.7 (CH), 71.5 (CH), 70.8 (CH_2), 69.5 (CH_2) ppm.

2,3,4,6,2',3',6'-Hepta-O-benzyl-4'-(dibenzyl phosphate)-α,α-D-trehalose (11)

To a cooled (0°C) solution of phosphorus trichloride (0.45 ml, 5.14 mmol) in diethyl ether (30 ml), triethylamine (2.3 ml, 16.4 mmol) was added dropwise. A solution of **10** (500 mg, 0.51 mmol) in diethyl ether (20 ml) was added. The reaction mixture was stirred for 30 min at 0°C, an subsequently for 2 days at room temperature. The reaction mixture was cooled to 0°C and benzyl alcohol (3.2 ml, 30.8 mmol) was added. The reaction mixture was stirred for 30 min at 0°C, and subsequently for 5 days at room temperature. Pyridine (5 ml, 62 mmol) and acetic anhydride (2.9 ml, 31 mmol) were then added, after which the reaction mixture was stirred for 1.5 h. The reaction mixture was cooled to 0°C and H_2O_2 (30% in H_2O, 5.1 ml) was added. The reaction mixture was stirred overnight at room temperature, and subsequently cooled to 0°C. Then $Na_2S_2O_3$ (10% in H_2O, 50 ml) was

added, followed by stirring for 30 min at 0°C. The mixture was transferred to a separation funnel. The organic phase was separated, after which the aqueous layer was extracted with CH_2Cl_2 (3 x 50 ml). The combined organic layers were dried over anhydrous Na_2SO_4. The drying agent was filtered and the filtrate was concentrated under reduced pressure. The crude product was purified through HPLC (gradient elution: 0.1 % NH_4OAc in H_2O/acetonitrile 5/95 to 0/100, column: Phenomenex Luna C18(2) (5 µm 220 x 31.20 mm)) giving the title compound **11** as a colorless oil in a yield of 23% (143 mg, 0.116 mmol).

ESMS [m/z (fragment, intensity), API-ES positive mode]: 1255.5 ($M+Na^+$, 100). HRMS (ESI-TOF): calculated for $C_{75}H_{77}NaO_{14}P^+$ $[M+Na]^+$ 1255.4949; found 1255.4920.

^{1}H NMR (400 MHz, Benzene-d_6) δ 7.33 – 7.26 (m, 4H), 7.20 – 7.14 (m, 6H), 7.12 – 6.84 (m, 35H), 5.35 (d, *J* = 3.5 Hz, 1H), 5.31 (d, *J* = 3.5 Hz, 1H), 4.90 – 4.65 (m, 10H), 4.55 – 4.42 (m, 5H), 4.40 – 4.21 (m, 8H), 3.84 – 3.74 (m, 2H), 3.68 (dd, *J* = 10.1, 9.0 Hz, 1H), 3.56 – 3.45 (m, 3H), 3.40 (dd, *J* = 9.6, 3.6 Hz, 1H) ppm.

^{31}P NMR (162 MHz, Benzene-d_6) δ 12.59 ppm.

^{13}C NMR (101 MHz, Benzene-d_6) δ 139.8 (C), 139.6 (C), 139.4 (C), 139.2 (C), 139.0 (C), 138.9 (C), 138.6 (C), 136.9 (C), 136.8 (C), 128.7 (CH), 128.7 (CH), 128.6 (CH), 128.6 (CH), 128.6 (CH), 128.6 (CH), 128.5 (CH), 128.4 (CH), 128.2 (CH), 128.1 (CH), 128.0 (CH), 128.0 (CH), 127.9 (CH), 127.8 (CH), 127.7 (CH), 127.7 (CH), 127.6 (CH), 127.3 (CH), 93.4 (CH), 92.9 (CH), 82.4 (CH), 80.2 (CH), 80.1 (CH), 80.1 (CH), 79.9 (CH), 78.6 (CH), 76.2 (CH), 76.1 (CH), 75.5 (CH_2), 75.0 (CH_2), 74.7 (CH_2), 73.7 (CH_2), 73.7 (CH_2), 73.3 (CH_2), 73.2 (CH_2), 71.8 (CH), 71.1 (d, *J* = 4.7 Hz, CH), 69.5 (CH_2), 69.4 (CH_2), 69.4 (d, *J* = 5.5 Hz, CH_2), 69.3 (d, J = 5.4 Hz, CH_2) ppm.

Trehalose-4-phosphate dipotassium salt tridecahydrate (12)

The general procedure as described for the synthesis of **7** was applied. This afforded the title compound **12** as a light brown powder with a yield of 79 % (65 mg, 0.89 mmol).

ESMS [m/z (fragment, intensity), API-ES negative mode]: 421.0 ($M\text{-}H^+$, 100). HRMS (ESI-TOF): calculated for $C_{12}H_{23}NaO_{14}P^+$ $[M+Na]^+$ 445.0723; found 445.0700.

^1H NMR (400 MHz, Deuterium Oxide) δ 5.10 (d, *J* = 3.8 Hz, 1H), 5.08 (d, *J* = 3.9 Hz, 1H), 3.92 (dd, *J* = 9.8, 8.2 Hz, 1H), 3.85 – 3.73 (m, 6H), 3.74 – 3.66 (m, 2H), 3.62 (dd, *J* = 9.8, 3.9 Hz, 1H), 3.53 (dd, *J* = 9.9, 3.8 Hz, 1H), 3.36 (t, *J* = 9.6 Hz, 1H) ppm.

^{31}P NMR (162 MHz, Deuterium Oxide) δ 4.35 ppm.

^{13}C NMR (101 MHz, Deuterium Oxide) δ 93.4 (CH), 93.3 (CH), 72.6 (CH), 72.5 (CH), 72.1 (CH), 72.1 (CH), 71.5 (d, *J* = 6.6 Hz, CH), 71.5 (CH), 71.2 (CH), 71.2 (CH), 69.7 (CH), 60.5 (CH_2), 60.4 (CH_2) ppm.

Supplementary Figures

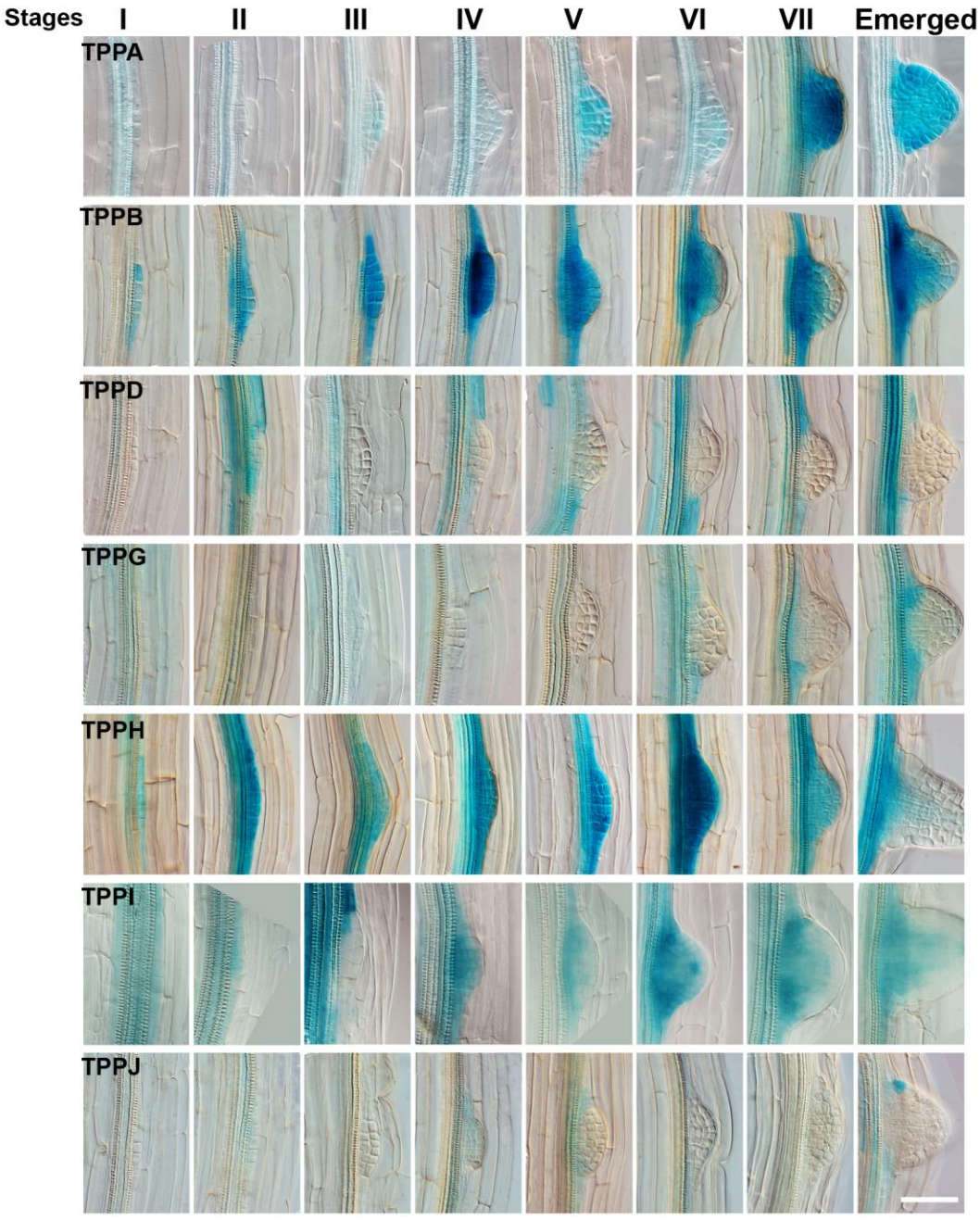

Figure S2. TPPA-J expression during lateral root development. Histochemical analysis of GUS activity in 6DAG transgenic Arabidopsis seedlings expressing GUS reporter gene driven by the respective native TPP promoter. The LR primordium stages were defined as described by Malamy and Benfey (1997) (*1*). Only TPP lines with detectable GUS- expression in LR primordium are shown. The bar indicates 100 µm.

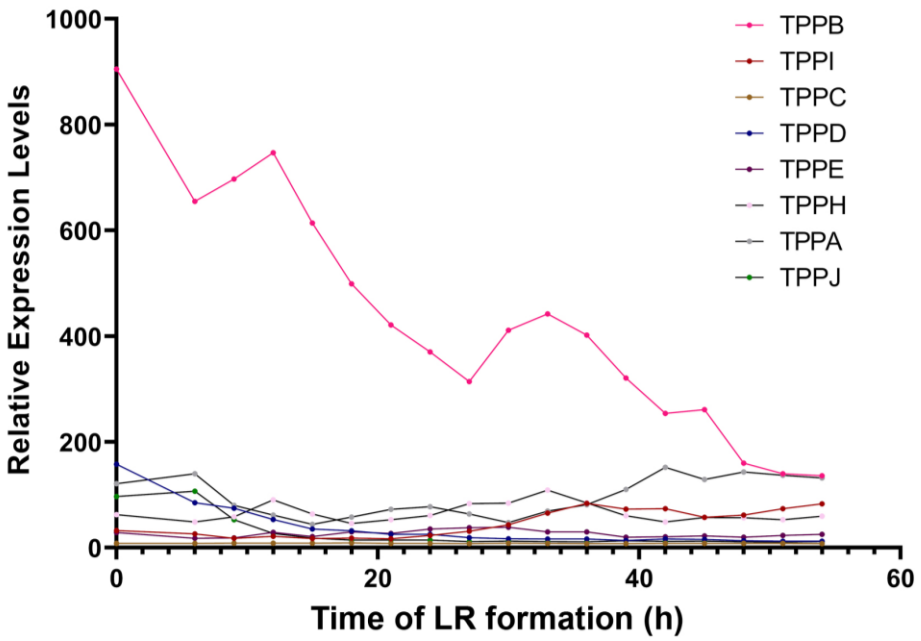

Figure S3: AtTPPA-J are expressed during LR formation. Expression levels of TPPA, *TPPB*, TPPC, TPPD, TPPE, TPPG, TPPH, TPPI and TPPJ during LR formation. Data was obtained from an updated VisuaLRTC version (*2*) and indicates the relative expression throughout the course of LR formation.

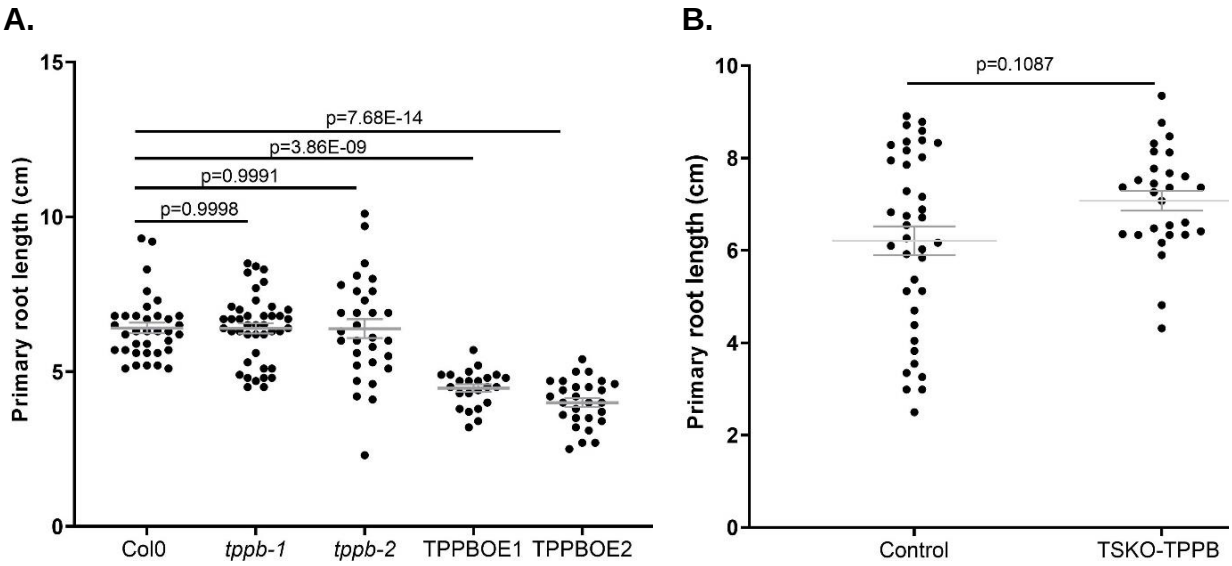

Figure S4: Primary root lengths of *TPPB* transgenic lines. Quantification of primary root length of 12 DAG wildtype (Col0), *tppb-1, tppb-2, TPPB*OE1 and *TPPB*OE2 (**A**) and TSKO-*TPPB* **(B)** seedlings grown on vertical plates. Dots represent individual datapoints and mean ±Standard Error of the Mean (SEM) are shown with lines and error bars, respectively. All analyses were done in three experimental replicates (n=23-42 seedlings). Significant differences between transgenic lines and Col0 were calculated by One-way-ANOVA with Dunnet's correction. Poisson regression was performed to obtain the p-value for B.

A.

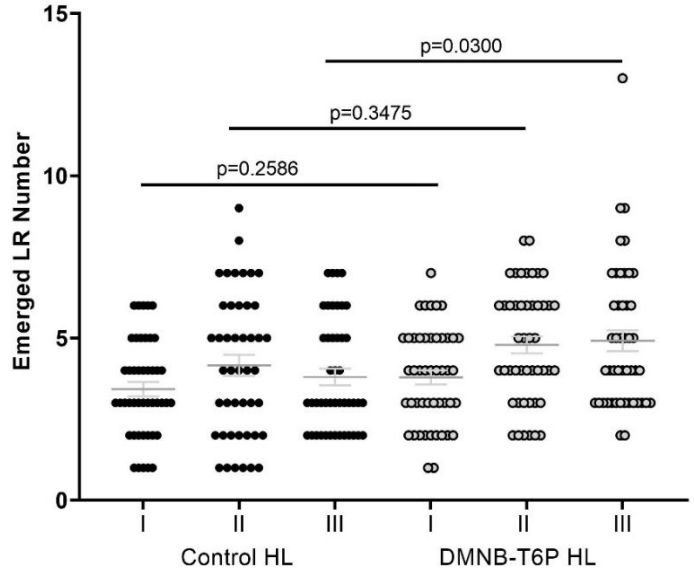

B.

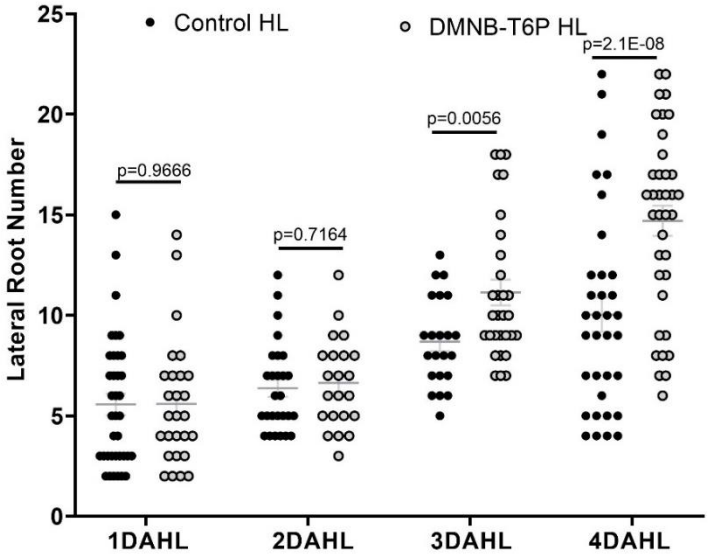

Figure S5: Treatment with DMNB-T6P results in LR formation A. Quantification of emerged LR number of the different plate sections (I,II,III) of 10 DAG Col0 seedlings that were transferred at 2 DAG to control (DMSO 0.1%) or DMNB-T6P (10nM) for 3 days and then exposed to high light (HL) treatment for 7 hours followed by growth under normal conditions for 4 days after HL (DAHL) (I, Root portion that developed before the transfer. II, Root portion that developed during the treatments. III, Root portion that developed after the high-light(HL) treatment). **B.** Quantification of LR primordium 1, 2, 3 and 4 days after HL (DAHL) based on histochemical detection of primordia using pCYCB1;1:GUS seedlings. Data indicates ± SEM of three experimental replicates (n=45 seedlings in A, n=22-30 seedlings in B). Significance of the differences between the control and DMNB-T6P treatment under the HL condition is calculated using Poisson regression for B with Dunnet's correction in A.

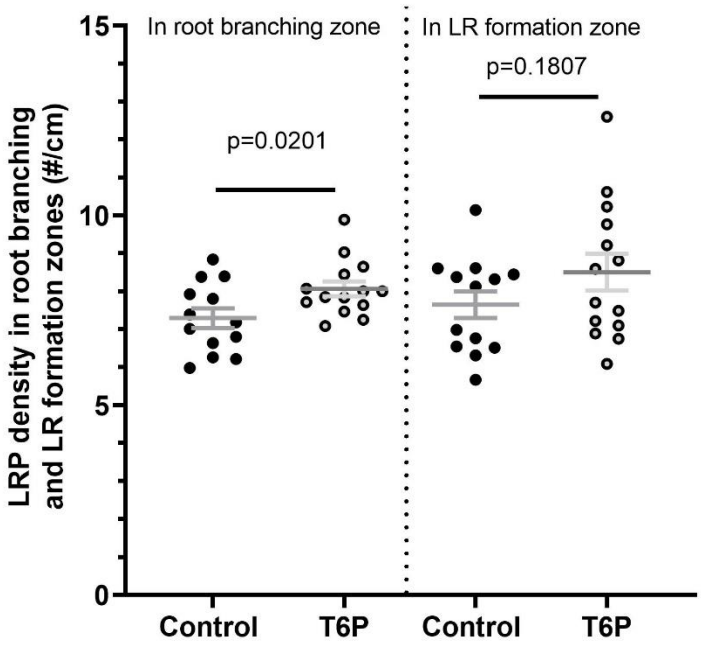

Figure S6: T6P-treatment induces LRP density in root branching zone. Quantification of LRP stages density in root branching and LR formation zones of 8 DAG wildtype seedlings (Col-0) transferred at 2DAG to control or T6P (1mM). p-values were obtained using Poisson regression (n=13).

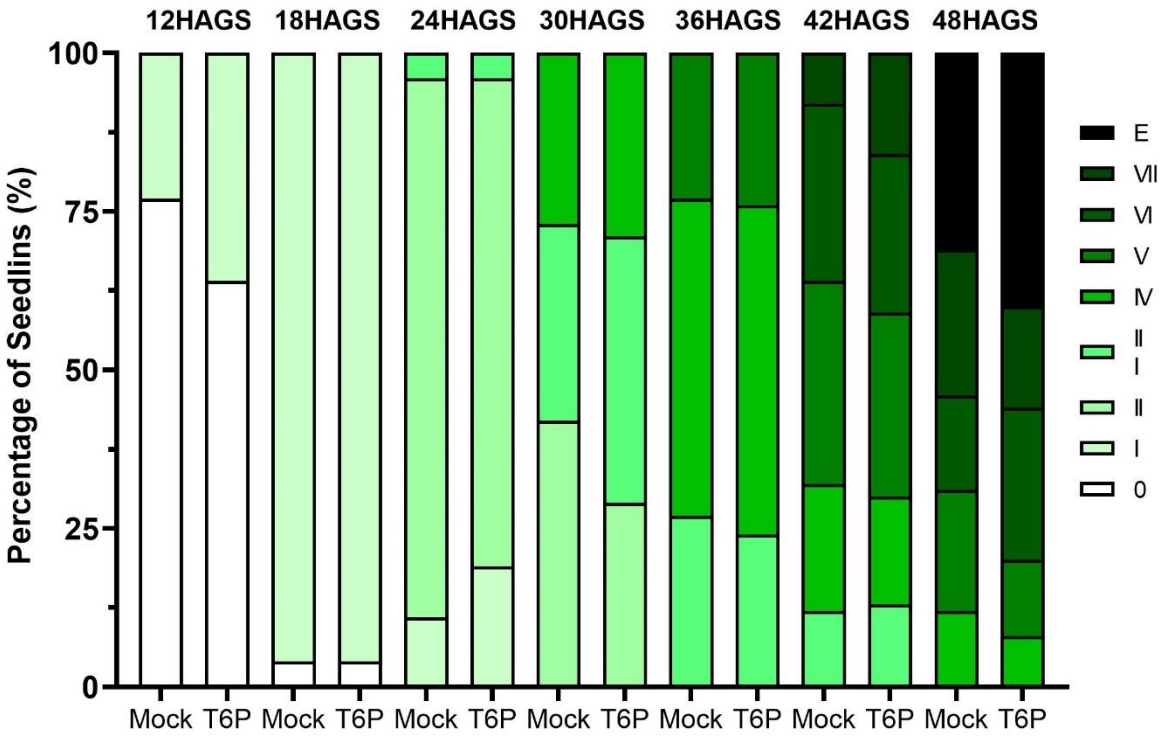

Figure S7: T6P treatment does not accelerate LRP development. 3DAG DR5:LUC seedlings, grown on 0.5xMS without sucrose, were transferred to medium with or without T6P (1mM), and after 2h the seedlings were gravistimulated (90° counterclockwise rotation). Quantification of the percentage of seedlings showing a certain LR primordium stage (1) was done 12, 18, 24, 30, 36, 42 and 48h after gravistimulation (HAGS). There are no statistically significant differences between treatments as determined via chi-square tests (n=30).

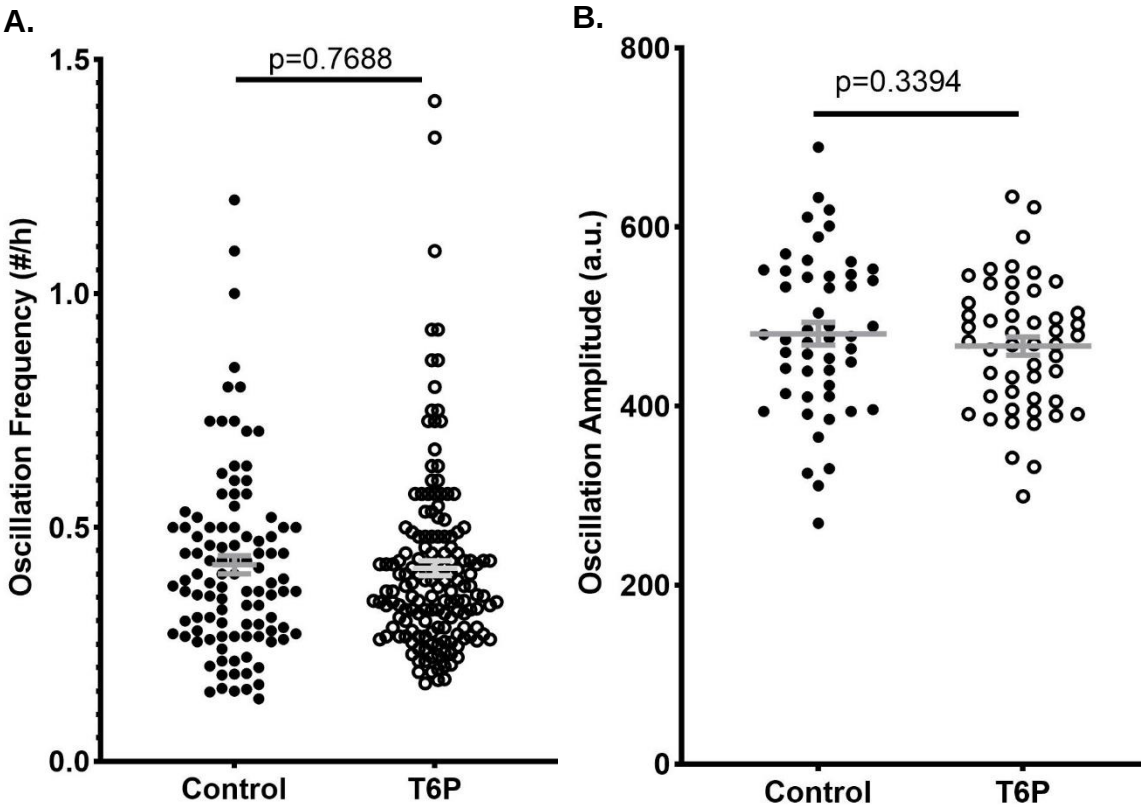

Figure S8: T6P treatment does not interfere with the oscillation patterns of pDR5:LUC. A. 3DAG *pDR5:LUC* seedlings were transferred to plates with or without 1mM T6P, sprayed with 1mM D-luciferin and incubated in the dark for 1h. *DR5:LUC* oscillation frequencies (A) and amplitudes (B) were determined via 22h time lapse assays. Lines indicate averages and error bars represent SEM of at least 100 oscillations. p-value was determined by T-tests

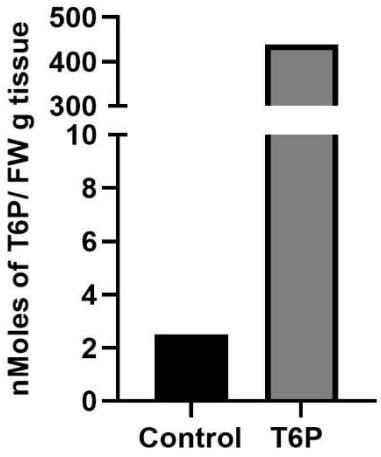

Figure S9: Exogenous T6P treatment increases T6P levels in roots. Measurements of T6P levels in root tissue of 8 DAG wildtype seedlings that were transferred at 5 DAG to control medium or T6P (1mM) containing medium for 3 days. The measurements were done by High Performance Liquid Chromatography equipped with a C-18 column and coupled to a Q Exactive Orbitrap mass spectrometer. Data represents one experimental replicate.

A.

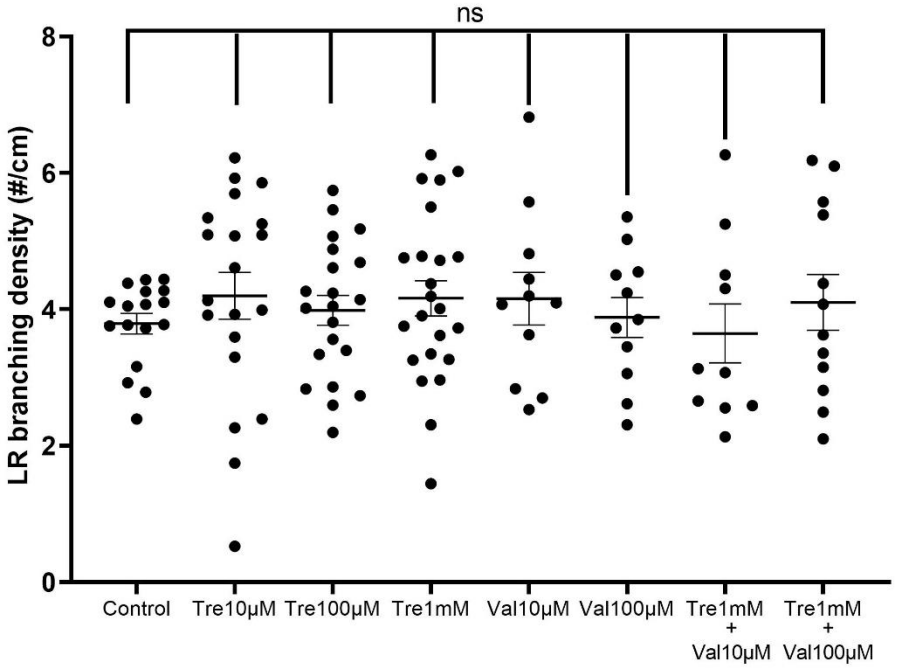

B.

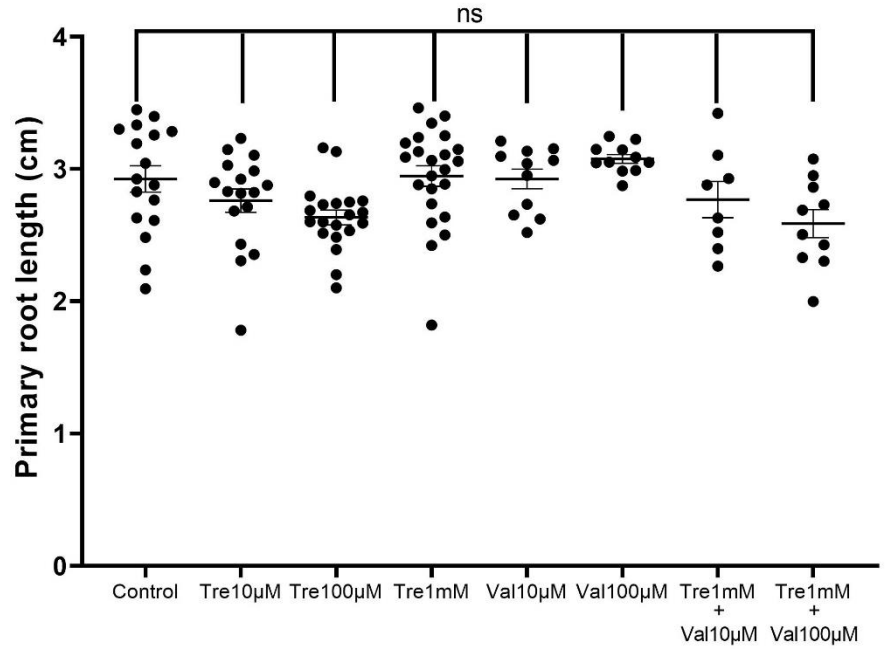

Figure S.10: Trehalose addition and validamycin treatment do not promote formation of new lateral roots. Quantification of emerged LR density of control, trehalose (Tre) and validamycin A (Val, trehalase inhibitor) treatments of 8 DAG seedlings. 2 DAG Col0 seedlings were transferred to 100µM or 1mM of T6P, 10µM, 100µM, 1 mM or 10 mM of trehalose, 10µM of Validamycin A or to the co-treatment of trehalose (1mM) and Validamycin A (10µM) in 0.5XMS solid medium without sucrose for 6 days. All data represent the average ± SEM of two experimental replicates. Significant differences from the control treatment were determined by one-way-ANOVA test.

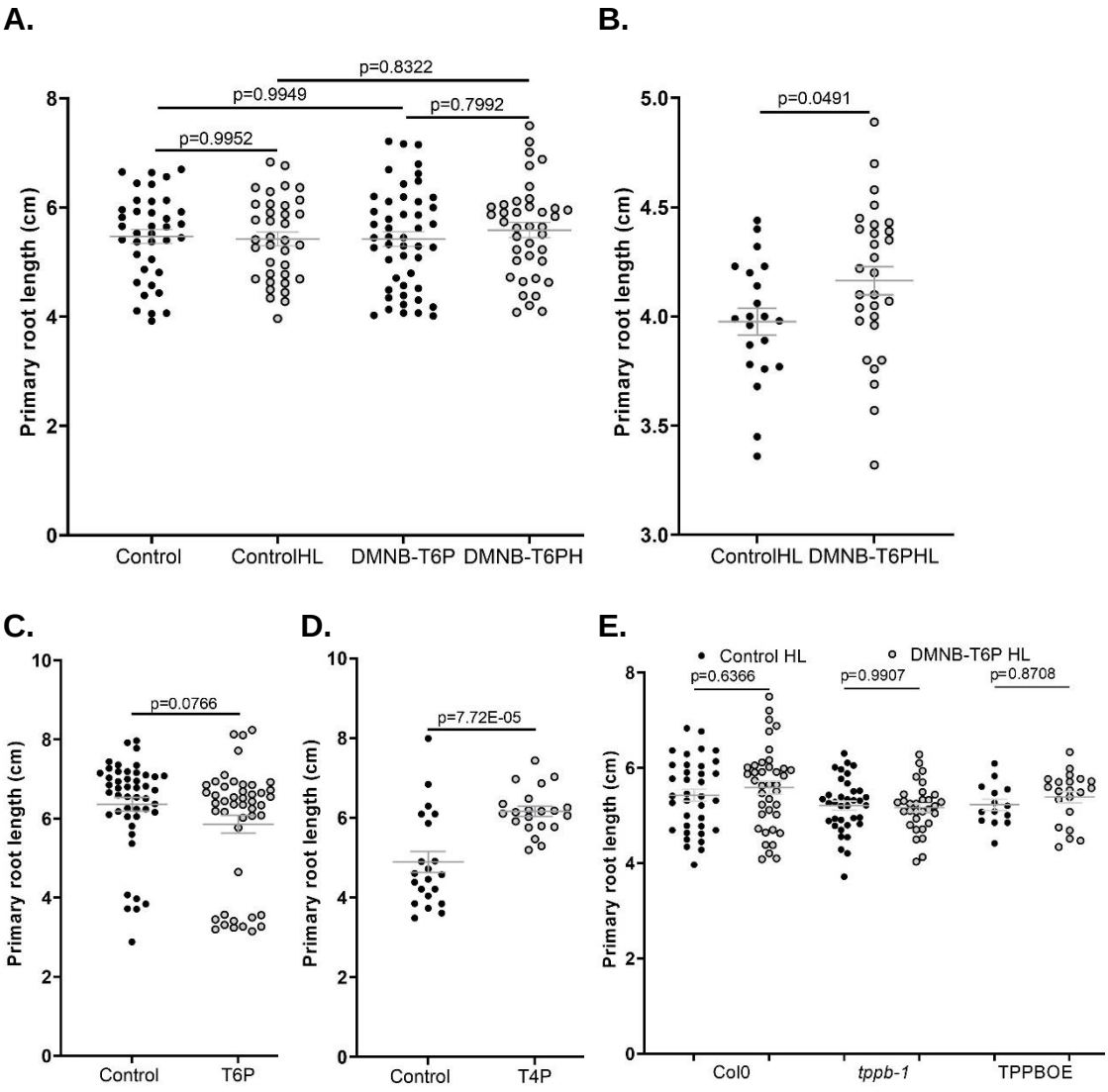

Figure S11: Primary root lengths of exogenous T6P treatments. A. Quantification of primary root lengths of 10 DAG Col0 seedlings treated as indicated in Fig. S5A. **B.** Primary root lengths of 9 DAG pCYCB1;1:GUS seedlings that were treated as indicated in Fig.S5A but quantified at 3 DAHL. **C.** Primary root length quantification of 12 DAG wildtype seedlings that were transferred at 2 DAG to standard growth medium or to medium containing T6P (1mM) or T4P (1mM) in **D.** Individual data and mean±SEM are shown for three experimental replicates (n=36-48). P-value was calculated using Poisson regression with Tukey's correction. Dots represent the individual data points; lines indicate mean and error bars from three experimental replicates (n=21-29). Poisson regression was used to calculate p-values. **D.** Average of primary root lengths of 10 DAG Col0, *TPPB*OE1 and *TPPB*-1 seedlings treated as in Fig.S6A. Means ±SEM are shown by lines and error bars, respectively, from three experimental replicates. Significant differences between treatments and control were obtained by one-way-ANOVA test with Tukey's correction in A and by T-Student's test in B-D. In the case of E, p-values were calculated using two-way-ANOVA test.

A.

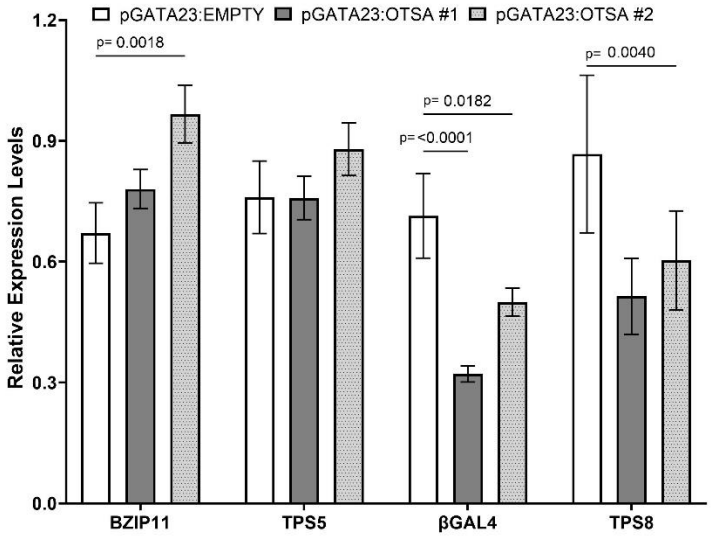

B.

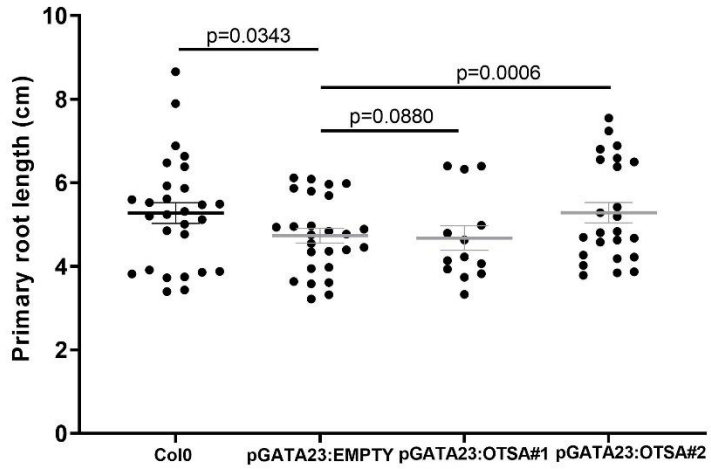

Figure S12: Characterization of p*GATA23*:otsA lines. A. Relative expression levels of SnRK1 marker genes in root tissue of 8 DAG p*GATA23*:empty, p*GATA23*:otsA#1 and p*GATA23*:otsA#2 seedlings (BZIP11 and TPS5 are down-regulated by SnRK1 and βGAL4 and TPS8 are up-regulated by SnRK1). **B.** Primary root length of 12 DAG Col0, p*GATA23*:empty, p*GATA23*:otsA#1 and p*GATA23*:otsA#2 seedlings grown on vertical plates. otsA relative transcription levels in root tissue of 8 DAG seedlings of Col0. Data represents three experimental replicates (n=14-27). Statistically significant differences between lines were determined via one-way-ANOVA with Dunnet's correction. Data represents the average ± SEM of three experimental replicates with three technical repeats. Statistical analysis was done using two-way-ANOVA test and p-values representing significant differences are shown.

A.

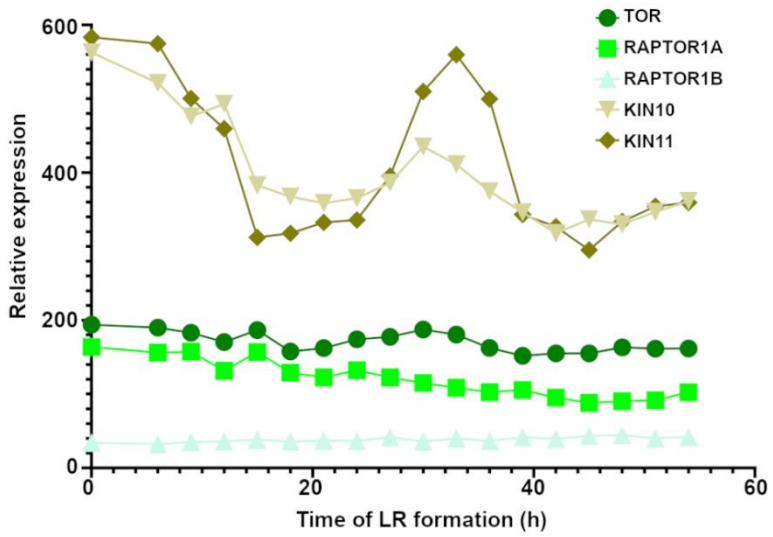

B.

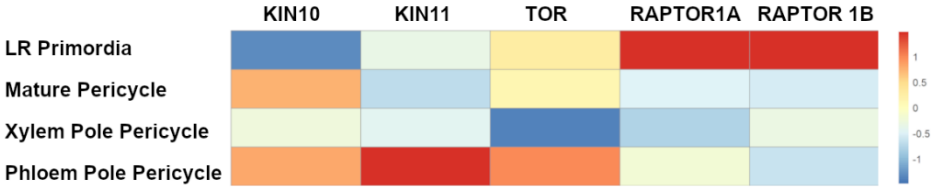

Figure S13: Subunits of SnRK1 and TOR- complexes are differentially regulated during LR formation. A. Expression pattern of *KIN10* and *KIN11*, catalytic subunits of SnRK1 complex and *TOR*, *RAPTOR1A*, *RAPTOR1B* and *LST8*, subunits of TOR complex during LR formation. These represent relative expression data obtained from an updated VisuaLRTC version (*2*). **B.** Heatmap (row-scaled) visualizing expression of *SnRK1* and *TOR* complex subunits in different pericycle cells based on a published single cell RNAseq study *(3)*.

A.

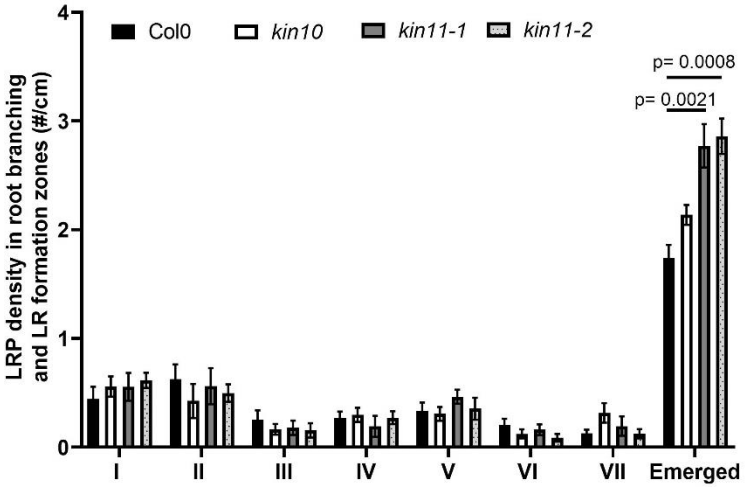

B.

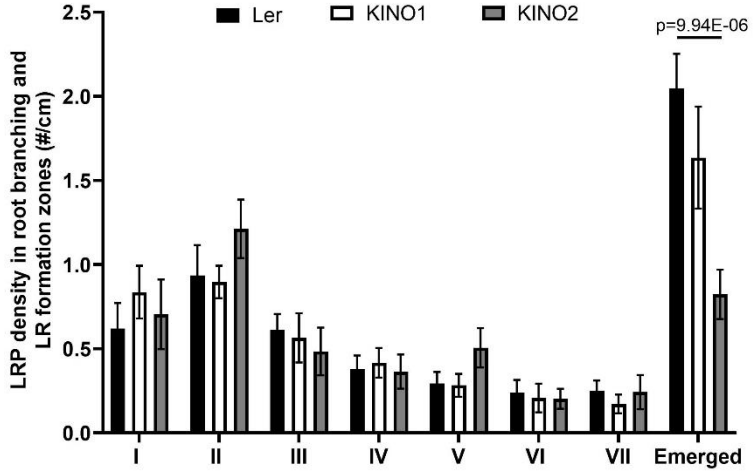

C.

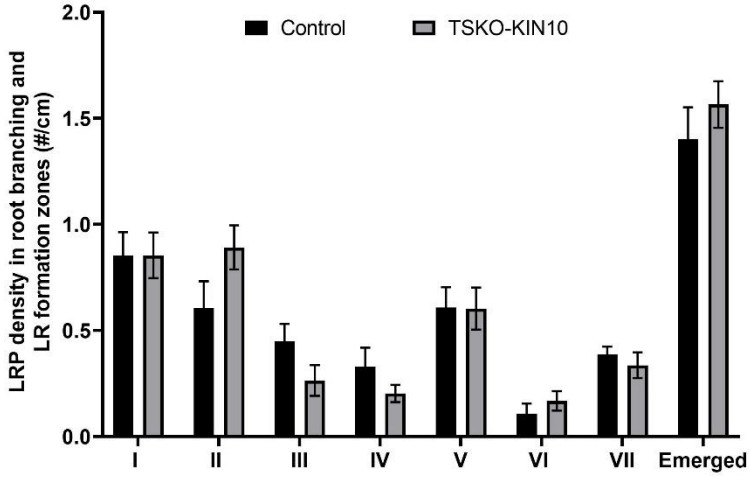

Figure S14: Characterization of lateral root development of SnRK1-complex transgenic lines. A. Staging of LR primordium in 8 DAG Col0, *kin10, kin11-1* and *kin11-2* seedlings. **B.** Staging of LR primordium in 8 DAG seedlings of Ler, KINO1 and KINO2. **C.** Staging of LR primordium in 8 DAG TSKO-KIN10 line #1 seedlings. Data represent the average ± SEM of two experimental replicates (n=12-16 seedlings). Statistically significant differences between lines were calculated by a Generalized Estimation Equations (GEE) model. We provide only p-values showing significant statistical difference.

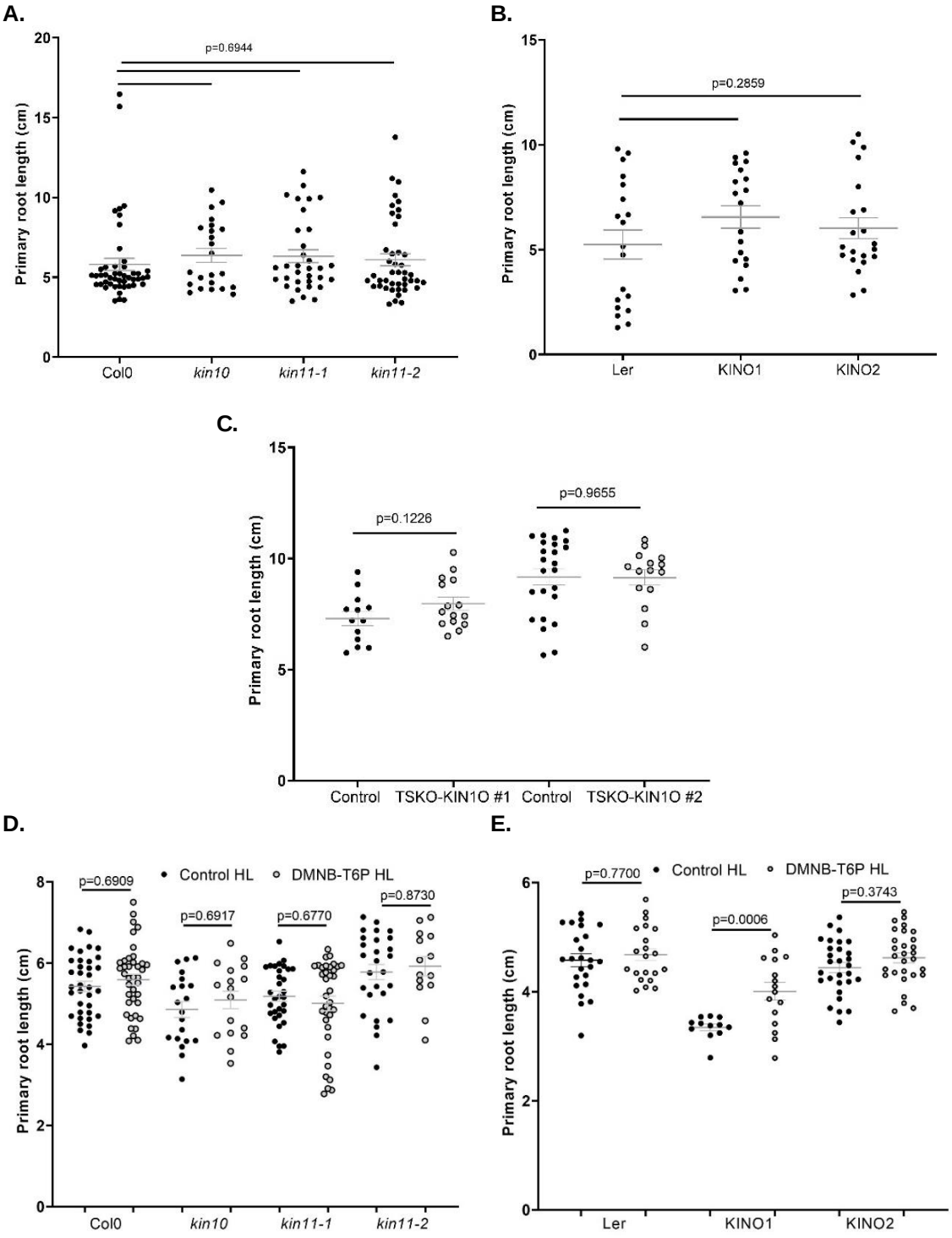

Figure S15: Primary root lengths of SnRK1-complex transgenic lines. A. Quantification of the primary root lengths of 12 DAG seedlings of Col0 (WT), mutants of the catalytic unit of SnrK1, KIN10 and KIN11: *kin10*, *kin11-1*, *kin11-2*, **B.** Ler (WT), and overexpressor lines of KIN10: KINO1 and KINO2 and **C.** TSKO-KIN10 seedlings grown in vertical plates. **D.** Primary root lengths quantification after 4 DAHL of 10 DAG Col-0, *kin10*, *kin11-1* and *kin11-2* and **E.** Ler, KINO1 and KINO2 seedlings treated as in Fig. S5A. Individual datapoints and means ± SEM are shown for at least two experimental replicates (n=13-49 seedlings). Statistical significances were determined via Kruskal-Wallis chi-squared for A., one-way-ANOVA for B, t-Student's test for C and two-way-ANOVA for D-E.

A.

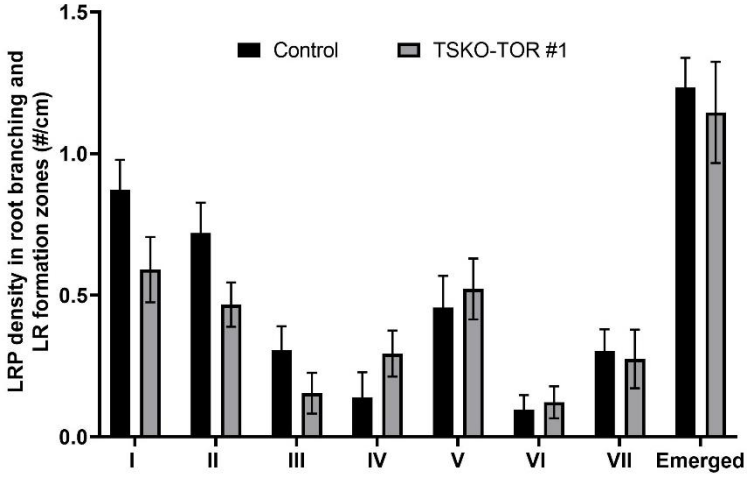

B.

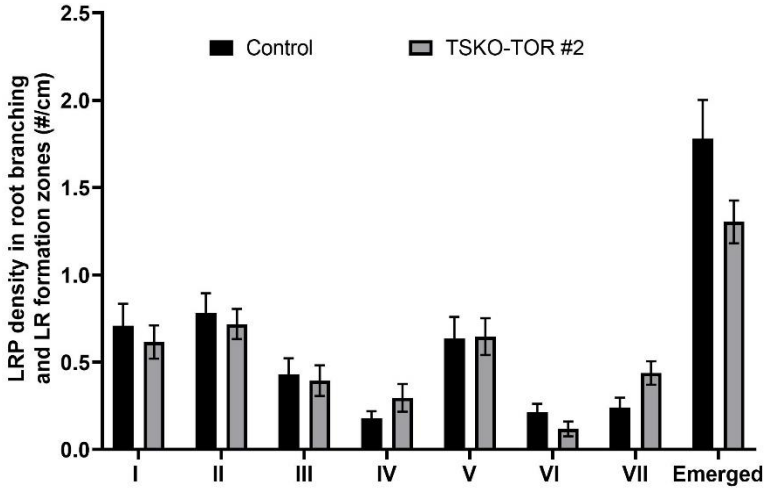

Figure S16: Characterization of lateral root development of TSKO-TOR transgenic lines. A. Staging of LR primordium in 8 DAG seedlings of TSKO-TOR seedlings line #1 or line #2 in **B.** Data represent the average ± SEM of two experimental replicates (n=12-16 seedlings). Statistically significant differences between lines were calculated by a Generalised Estimation Equations (GEE) model. We only provided p-values that represent a significant statistical difference.

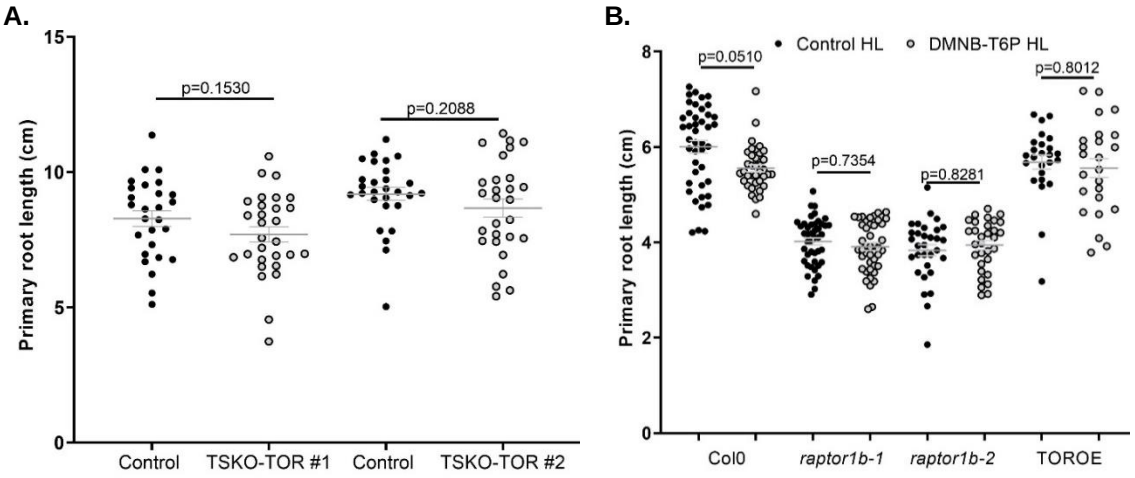

Figure S17: Primary root lengths of TOR-complex transgenic lines. A. Quantification of the primary root lengths of 12 DAG seedlings of Col0 (WT) and TSKO-TOR transgenic lines seedlings grown in vertical plates. **B.** Average of primary root lengths after 4 DAHL of 10 DAG Col-0, *raptor1b-1, raptor1b-2* and TOROE seedlings treated as in Fig. S5A. Individual datapoints and means ± SEM are shown (n=17-43) for three experimental replicates. Statistical significances were determined via one-way-ANOVA for A and via two-way-ANOVA with Dunnet's correction for B.

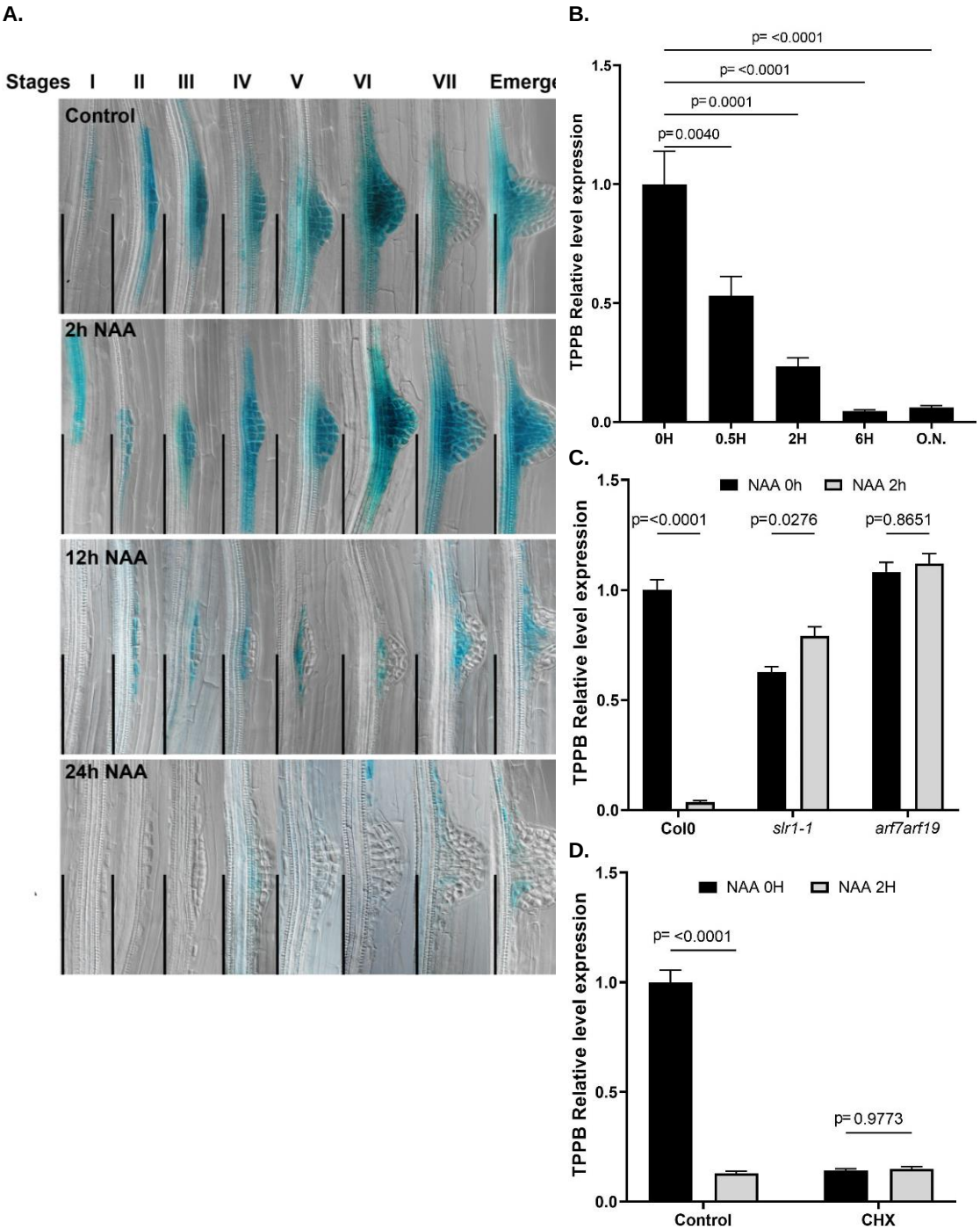

Figure S18: *TPPB* is downregulated by auxin in LR cells. A. Histochemical analysis of GUS activity in 6DAG p*TPPB*:GUS seedlings treated for 2h, 12h or 24h with 10µM NAA. LR primordium stages were defined as indicated by Malamy and Benfey (1997) *(1)*. The scale bar indicates 100µm. **B.** Relative expression of *TPPB* in Col0 roots of 5 DAG seedlings treated with 10µM NAA for 0.5h, 2h, 6h or overnight (ON). **C.** *TPPB* relative expression in Col0, *slr1-1* and *arf7arf19* 5 DAG roots treated with 10µM NAA for 6 h compared to control treatment (0.1% DMSO). **D.** Relative *TPPB* expression on Col0 roots treated for 2 hours with 10 µM NAA and pretreated 30 minutes with 50µM CHX. All analyses were done in triplicate. Significant differences from control treatment were determined by two-way-ANOVA.

Table S1. Genotyping primers.

Mutant	**Forward(5'→3')**	**Reverse(5'→3')**
TPPB-1	GTGCGGAAAAATGAAATATCG	TTCAATCATTGGACGGATTTC
TPPB-2	CAAGAAAGTGAACAAAGGAAAGG	TTTGTAACAGAGATGGCCTGC
kin10	CCTCTAGTGGTTATCTCGGGG	AAAATCAATCTTGGTGGCATG
kin11-1	CGTAGTGATCCACATGTGCAG	GATTGCAGACTTTGGGTTGAG
kin11-2	TGCGGTTTGATGATTATAATCG	TCGATTCCACTCCATTATTGC
TOROE	TTGTAACAACGGAGAAACACG	CAAAAGATTGCGACGAGGTAG
LBb1.3	ATTTTGCCGATTTCGGAAC	
p35Sf	TCTACCTGGGGGTGGGTGCTCC	
p*TPPB*cds-r		GTCTTTTACGACTTCTCTCATCTC
p*GATA23*F	ACTTTGCTTTCCACCCGACA	

Table S2. Gene accession numbers.

Gene	Accession Number
ARF7	AT5G20730
ARF19	AT1G19220
IAA14	AT4G14550
TPPB	AT1G78090
TPS5	AT4G17770
TPS8	AT1G70290
BZIP11	AT4G34590
BGAL	AT5G56870
UDPGDH	AT3G47340
ASN	AT3G29360
RAPTOR1B	AT3G08850
LST8	AT3G18140
RAPTOR1A	AT5G01770
TOR	AT1G50030
CDKA1	AT3G48750
EEF1α4	AT1G30230
UBI10	AT3G53090
PP2A	AT1G69960
TPPA	AT5G51460
TPPD	AT1G35910
TPPE	AT2G22190
TPPF	AT4G12430
TPPG	AT4G22590
TPPH	AT4G39770
TPPI	AT5G10100
TPPJ	AT5G65140
KIN10	AT3G01090
KIN11	AT3G29160
GATA23	AT5G26930
OTSA	EG11751

Table S3. Cloning primers.

Primer	Sequence (5'→3')
OTSA-attB1	GGGGACAAGTTTGTACAAAAAAGCAGGCTACATGAGTCGTTTAGTCGTAGTATCTAA
OTSA-attB2	GGGGACCACTTTGTACAAGAAAGCTGGGTTCTACGCAAGCTTTGGAAAGGTA

Table S4. qRT-PCR primers Gene

Gene	Forward(5'→3')	Reverse(5'→3')
TPPB	GATGAGAAGAGATGGCCTGC	CCCTTGTCCCATTTGATTGT
TPS5	TCTCGGTTTGGGTGCAGAGCA	ACCAAACTCGACGTTTCCCAGTCT
TPS8	TGTCGTCGAGGGACCAACTA	TAGCCACTACCGTCGGATGA
BZIP11	TGGGCATGTGTTCGAACCCTCT	AGACGCCATGAGAGGCTGGT
BGAL	ACTCAGGAACATGGGACATGTCGA	TCCTTGAGTCCATCTCACACCGGA
UDPGDH	TCCACCATCACCGAACCTG	CAGACAGAGATGAGCGAGTG
ASN	GAACCCATCGGACGTCGTAA	GAACCCATCGGACGTCGTAA
RAPTOR1B	CGGAGCAGTTACCTATTGTTCT	ACAGCCCATGAACCCATATC
LST8	ACCAGAAGTCGGTACACCTAT	ACAAGGAGCGCCATACATAAC
RAPTOR1A	GGCGTGTGCTTTCTGTTATTG	GAGGAGTGTGAGATGCTGATG
TOR	TTACTCCTTCCGGCACTTATTC	ACCTGAACACACGGGATTAC
CDKA1	ATTGCGTATTGCCACTCTCATAGG	TCCTGACAGGGATACCGAATGC
EEF1α4	CTGGAGGTTTTGAGGCTGGTAT	CCAAGGGTGAAAGCAAGAAGA
UBI10	ACGAGCAAGCACTATGAGGG	ACACACTGTTTACACCAGCCT
PP2A	TTGGTGCTCAGATGAGGGAGAG	TTCACCAGCTGAAAGTCGCTTAG
OTSA	CCCGATCGGCATTGAACCG	CCAGCCGTTCGACAGAAAAG

References

1. J. E. Malamy, P. N. Benfey, Organization and cell differentiation in lateral roots of Arabidopsis thaliana. *Development*. **124**, 33–44 (1997).

2. B. Parizot, B. de Rybel, T. Beeckman, VisuaLRTC: A new view on lateral root initiation by combining specific transcriptome data sets. *Plant Physiol.* **153**, 34–40 (2010).

3. HP. Gala *et al.,* A single-cell view of the transcriptome during lateral root initiation in Arabidopsis thaliana. *The Plant Cell*. **33(7)**, 2197–2220 (2021).